Determination of the Boltzmann constant with an acoustic quasi-spherical resonator filled with argon

Arnaud Guillou, Laurent Pitre, Fernando Sparasci, Daniel Truong, Lara Risegari, Marc Himbert

ACOUSTICS 2012

Determination of the Boltzmann constant with an acoustic quasi-spherical resonator filled with argon

A. Guillou, L. Pitre, F. Sparasci, D. Truong, L. Risegari and M. E. Himbert

Laboratoire Commun de Métrologie, 61 rue du Landy, 93210 La Plaine Saint Denis, France
arnaud.guillou@cnam.fr

There is an important interest in the international metrology community for new accurate determinations of the Boltzmann constant k_B, in order to redefine the unit of thermodynamic temperature, the kelvin. The value of the Boltzmann constant is linked to the speed of sound c in a noble gas. The method described here consists in measuring u inside a quasi-spherical acoustic resonator of inner volume of 0.5 L filled with argon, during an isotherm process at the temperature of the triple point of water (273.16 K) from 0.05 MPa to 0.7 MPa.
The determination of k_B at LNE-CNAM with this technique allowed us to obtain the value $k_B = 1.38064774\ (171)\cdot 10^{-23}\ \mathrm{J}\cdot\mathrm{K}^{-1}$, i.e. with a relative uncertainty of $1.24\ \cdot 10^{-6}$.
In this paper, we present the acoustical model use at LNE-CNAM. Moreover, we focus on the parameters of the experiment which have an effect on the measurement of u with this method (like gas purity, static pressure, etc) and how they were carefully controlled to get the lowest uncertainty on k_B up to now.

1 Introduction

The current definition of the unit of thermodynamic temperature (kelvin) is linked to a natural property of water obtained at the temperature of it triple point $T_{TPW} = 273.16$ K [1]. The 23rd General Conference of Weights and Measures (CGPM) recommended redefining some base units of the International System of Units (SI) with fundamental constants of physics [1]. In this context, the kelvin could be redefined by fixing experimentally, with a relative uncertainty of $1\ \cdot 10^{-6}$, the value of the Boltzmann constant k_B.
The Boltzmann constant is defined as $k_B = R/N_A$, where R is the gas constant and N_A the Avogadro constant.
Furthermore, k_B can be related to the zero pressure limit of the speed of sound, u, in a gas at the temperature T, as

$$k_B = \frac{M}{\gamma_0 T_{TPW} N_A} \lim_{P\to 0}^{*} u^2(P, T_{TPW}) \tag{1}$$

where $u^2(P, T_{TPW})$ is the square of the speed of sound at a pressure P and at the temperature of the triple point of water, T_{TPW}. M is the molar mass of the gas, $\gamma_0 = Cp/Cv$ is the ratio of the specific heat capacities for dilute monatomic gases. The term $\lim^{*}_{P\to 0}$ indicates that we estimate the terms independent of the pressure in $u^2(P, T_{TPW})$.
Nowadays, the technique which allows getting an accurate determination of k_B is the acoustic method developped at LNE-CNAM which consists in measuring u in a quasi-spherical volume filled with argon [2]; technique which is described in this paper.
In the first section, the acoustical model is presented. We focus particulary on the correction which are applied during the frequency measurements of radial modes within a quasi-spherical cavity. The second section deals with the experimental apparatus used at LNE-CNAM. In a last section, we present the data analysis.

2 Acoustical model

The speed of sound u can be determined by measuring the resonant frequencies f_{ln} within a known radius spherical cavity. The basic equation of this experiment is given by

$$u = \frac{2\pi\, a}{z_{ln}} f_{ln} \tag{2}$$

where a is the radius of the cavity and $z_{ln} = k_{ln}a$ is the n$^{\text{th}}$ root of $j'_l(z) = 0$, with $j_l(z)$ the spherical Bessel function of order l.
For practical purposes, we can't measure directly f_{ln}. Indeed the physical quantity measured is a complex frequency defined as

$$F_{ln} = f_{ln} + \Delta f_{ln} + i\, g_{ln} \tag{3}$$

where Δf_{ln} is the frequency shift and g_{ln} is the half-width of the resonant curve due to the disruptive and dissipative physical effects and/or elements which take place within the resonator.
These two terms are summed up in the next subsections. Six effects compose the acoustic model and are labeled by:

- the thermal boundary layers Eq.(6);
- the bulk losses Eq.(9);
- the perturbation on the wall of the resonator (microphones Eq.(12) and tubes Eq.(13));
- the shell vibrations Eq.(15);
- the inner shape of the resonator (tri-axial form) Eq.(14).

Only radial modes from 4000 Hz to 26000 Hz (modes 02-05, 08 and 09) are studied in this work. The speed of sound measurements are made in argon at the temperature of the triple point of water $T_{TPW} = 273.16$ K. To obtain the zero pressure limit of u^2, an isotherm is realized for static pressures from 0.05 MPa to 0.7 MPa; then an extrapolation to the zero pressure limit is made.

2.1 Thermal boundary layers

The specific admittance β_w of the acoustic resonator wall has an admittance which is defined, for radial mode $0n$ frequencies, as

$$\beta_w = (1+i)\frac{\gamma-1}{2}\delta_t\frac{\omega}{u} \tag{4}$$

with δ_t, the thermal layer thickness expressed as

$$\delta_t = \sqrt{\frac{2\lambda}{\rho\, C_p\, \omega}} \tag{5}$$

where λ is the thermal conductivity coefficient, ρ is the gas density and $\omega = 2\pi f$ [3].
This thermal boundary layer yields a frequency shift Δf_{0n}^{TBL} and contributes to the resonant half width peak g_{0n}^{TBL} by

$$\frac{\Delta f_{0n}^{TBL} + i\, g_{0n}^{TBL}}{f_{0n}} = i\frac{u}{2\pi a}\beta_w = (i-1)\frac{(\gamma-1)}{2}\frac{\delta_t}{a}. \tag{6}$$

This effect is the one which generates the larger corrections in the acoustical model. As shown in the subsection 2.6, more than 80% of the final correction is due to this effect ; its contributions, at $P = 0.1$ MPa, are $(-250 + i\,50)$ ppm $< (\Delta f_{0n}^{TBL} + i\, g_{0n}^{TBL})/f_{0n} < (-50 + i\,250)$ ppm. In other words, a good estimation of the impact of the thermal boundary layer on the acoustic measurements allows to correctly determine

the speed of sound in the gas.
Eq.(6) is right assuming that the temperatures of the gas and the resonator shell are equal at the interface. At low static pressure P, we have to take in account a discontinuity of the temperature in the boundary condition [4], even if this will create a frequency shift of an amount below 1 ppm. This frequency shift is given by

$$\frac{\Delta f^{TBL'}}{f_{0n}} = \frac{(\gamma-1)}{a} l_{th}. \tag{7}$$

where l_{th} is the thermal accommodation length defined as

$$l_{th} = \frac{\lambda}{P}\sqrt{\frac{\pi M T}{2R}}\frac{2-h}{h} \tag{8}$$

where $0 < h \leq 1$ is the thermal accommodation coefficent. This coefficient is linked to the gas ability being at equilibrium with the resonator wall and depends of four factors:

- the rugosity of the inner resonator surface;
- the wall resonator composition;
- the gas composition;
- the wall temperature.

In this work, h was estimated experimentally as 0.782 [2], which is in agreement with h values found in the experimental studies reported in [5].

2.2 Gas bulk losses

The second effect is the dissipation due to the bulk attenuation of sound. This effect only contributes to the widening of the resonant peak. This widening is given by

$$\frac{g_{0n}^{BULK}}{f_{0n}} = \left(\frac{\pi f_{0n}}{u}\right)^2 \times \left((\gamma-1)\delta_t^2 + \frac{4}{3}\delta_v^2\right), \tag{9}$$

with δ_v, the viscious layer thickness defined as

$$\delta_v = \sqrt{\frac{2\mu}{\rho\,\omega}} \tag{10}$$

where μ is the dynamic viscosity of the gas.
This effect is larger at low pressures and increases with frequency. At $P = 0.1$ MPa, on the frequency span studied, the contribution of halfwidth of this effect is 5 ppm $< g_{0n}^{BULK}/f_{0n} <$ 20 ppm.

2.3 Perturbations of the inner resonator surface

Two acoustical transducers and also two capillary tubes are flush-mounted on the inner wall of the resonator. These four elements change the local wall admittance which influence the resonant frequency measurements [6]. These effects are defined as

$$\frac{\Delta f_{0n} + i g_{0n}}{f_{0n}} = i\frac{\beta_e\, S_e}{S_p\, \nu_{0n}}, \tag{11}$$

where β_e is the acoustic admittance of the element (microphone or tube), S_e and S_p are the surface of the element and the surface of the inner resonator wall.
The microphone presence induces a frequency shift of -4 ppm to 4 ppm ; the shift due to the tubes lies between -1 ppm and 1 ppm. The both have a contribution on the half peak widening about 0.5 ppm to 4 ppm.

2.3.1 Microphones

Recent researches at LNE-CNAM, in collaboration with the *Istituto Nazionale di Ricerca Metrologica* (INRiM, Italy) and also with the *Laboratoire Acoustique de l Université du Maine* (LAUM, France) allowed obtaining an accurate knowledge about the microphone influence during the measurements [7]. This experimental and theoretical study, based on the complex electrostatic transducer model [8], has allowed defining more precisely the frequency shift Δf^M and the energetic losses represented by g^M.
This model takes into account the strong coupling which exists between the gas and the membrane microphone, effect which was neglected in a previous model [3].
Thus, Δf_{0n}^M and g_{0n}^M due to the presence of two microphones flush-mounted on the resonator wall are defined as

$$\frac{\Delta f_{0n}^M + i g_{0n}^M}{f_{0n}} = 2 \times \frac{i\rho c Y_{a,M}}{S_p z_{0n}}, \tag{12}$$

where $Y_{a,M}$ is the input acoustic membrane admittance, detailled in [7].

2.3.2 Capillary Tubes

The gas purity needs to be controlled in order to obtain perfect condition for measuring u in pure argon. This can be made using a continous gas flow through the resonator. Two capillary tubes mounted on the resonator wall, one as inlet the other one as outlet, allow this gas renewal. However, this will disturb the wall impedance β_w. This effect was well studied in [9].
Carrying on Eq.11 and substituting $\beta_e S_e$ by $\rho u/Z_{tube}$, it yields

$$\frac{\Delta f_{0n}^{tube} + i g_{0n}^{tube}}{f_{0n}} = \frac{i\,\rho\,u}{S_p\, z_{0n}\, Z_{tube}}, \tag{13}$$

where Z_{tube} is the input acoustic tube impedance. Z_{tube} is estimated using an electro-acoustical analogy [6].

2.4 Tri-axial inner shape

The resonateur used and described in section 3 doesn't have an equal radius, as showned in Fig.4. These radius changes shift the resonant frequency, which was estimated by Mehl [10]. The second order perturbation correction, for the radial mode, is given by

$$\frac{\Delta f_{0n}^{TAE}}{f_{0n}} = \frac{4}{135} z_{0n}^2 \left(\varepsilon_1^2 - \varepsilon_1\varepsilon_2 + \varepsilon_2^2\right) \tag{14}$$

This effect depends only of the excentricities ε_1 and ε_2. It increases with the frequency and takes value between 0.5 ppm $< \Delta f_{0n}^{TAE}/f_{0n} <$ 10 ppm.

2.5 Correction of the shell vibrations due to the shell breathing mode

Near shell resonances, there is a strong coupling between the gas and the resonator wall. Shell movements could be small, however, these vibrations will interact with the gas, and cannot be neglected.
Vibrations are maximal when the resonant bulk frequency f_{0n} is near the resonant shell frequency f_{shell}. The theoretical model used to estimate the shell vibration amplitude is the

one which predicts elastic deformations of isotropic materials.
In the particular case of the breathing shell mode (vibrations are only function of the sphere radius), the frequency shift is defined as

$$\frac{\Delta f^{breath}}{f_{0n}} \approx -\frac{\kappa P}{1-(f_{0n}/f_{breath})^2} \tag{15}$$

with

$$\kappa = \frac{5\,a}{6\,t\rho_{shell}\,u_{shell}^2} \tag{16}$$

where t is the shell thickness, ρ_{shell} and u_{shell} are respectiveley the density and the longitudinal speed of sound of the shell [11].
For a resonator of radius a = 0.05 m and thickness t = 10 mm, the frequency of the breathing mode is estimated at f_{breath} = 15886.6 Hz [12].
The frequency shift will be larger when f_{0n} will be close to f_{breath}. This is one of the experimental limits: because of large shell vibrations, only modes for $|f_{0n}/f_{breath} - 1| > 0.02$ are kept. For exemple, the frequency shift due to this effect on the mode 02 ($f_{02} \approx 4400$ Hz) is below 20 ppm while for the mode 05 ($f_{05} \approx 13785$ Hz), the frequency shift can rise until 70 ppm. Also, this effect is more important at high static pressure because of an easier coupling between the gas and the shell.

2.6 Contribution of the disruptive effects in the acoustical model

Figure 1 and Figure 2 show the contribution in the acoustical model of each effect presented in this section. We can see in both figures, the importance of a good estimation of the thermal boundary layers impact on the measurement of u, presented in the subsection 2.1.

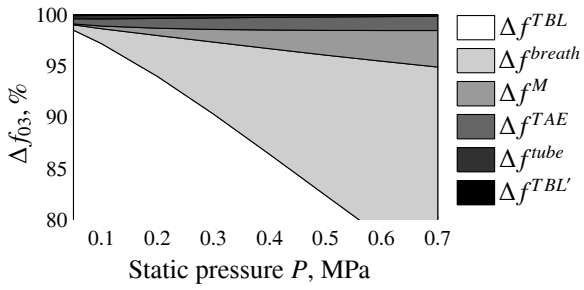

Figure 1: Effect contributions on the total frequency shift Δf_{03}

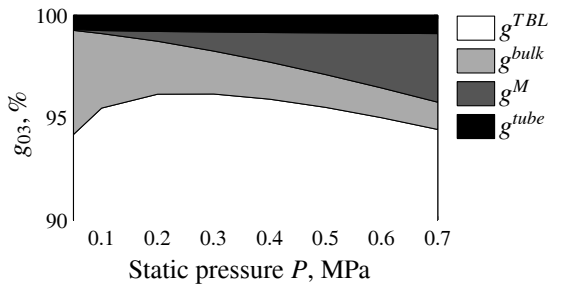

Figure 2: Effect contributions on the widening g_{03} of the resonant pic

3 Apparatus presentation

3.1 The quasi-spherical resonator BCU3

The acoustical resonator used at present at LNE-CNAM, named BCU3, is a 0.5 L quasi-spherical cavity assembled by two hemispheres made of copper as shown in Figure 3.

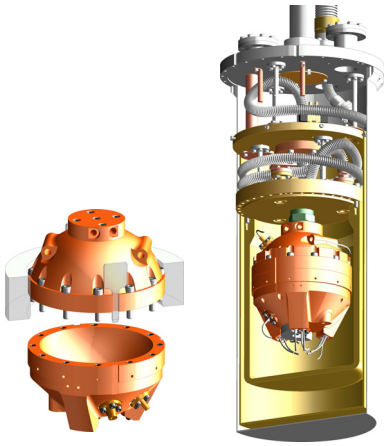

Figure 3: 3D views of BCU3 (left) and BCU3 inside it cryostat (right)

The inner shape isn't spherical and is designed as a triaxial ellipsoid form, which is defined as

$$\frac{x^2}{a^2} + \frac{y^2}{a^2(1+\varepsilon_1)^2} + \frac{z^2}{a^2(1+\varepsilon_2)^2} = 1, \tag{17}$$

where ε_1 and ε_2 are excentricities of order 0.001 and 0.0005 respectively, $a = a_{eq}/\sqrt{(1+\varepsilon_1)(1+\varepsilon_2)}$, with a_{eq} is the equivalent radius of a perfect sphere of equal volume.
This inner shape has been controlled using a Coordinate Measurement Machine (CMM) [13] and is showed in Figure 4. Absolute deviations between the designed features and the practical realization are less than 3 μm. These good agreements were obtained thank the final machining which was realized with diamond turning.

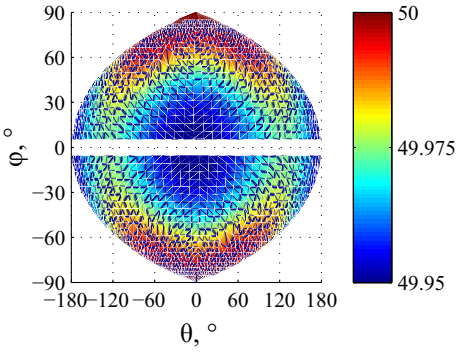

Figure 4: Winkel-Tripel projection of the inner BCU3 radius mesured with CMM

To determine u by measuring the resonant frequency of the cavity, we need to know the radius a_{eq} (Eq.2). The more accurate method to estimate the equivalent radius volume and the excentricities is the electromagnetic spectroscopy of the bulk [2]. Using this technique, it was find a_{eq} = 49975.095 μm with an uncertainty $u(a_{eq})$ = 0.014 μm. Also, the excentricities were determined: ε_1 = 0.001078 and ε_2 = 0.000506.

3.2 The acoustic BCU3 instrumentation

The resonator is equipped of two microphones; one is used as transmitter, the other as receiver. Both are 1/4 inch B&K microphones (type 4939). Their positions are optimized to get a mesurement of the radial mode frequencies which are the less disturbed by couplings with non-radial modes [2].
The acoustic source is driven from a frequency generator (SRS DS335) locked to a rubidium clock (SRS SIM940). Short frequency sweeps around resonant frequencies are emitted. At each frequency step, the signal from the receiver microphone is analysed with a lock in amplifier (SRS 830). All the equipment is controlled, and data are acquired, using a home-made software which runs under LabVIEW.

3.3 Control of the temperature, the pressure and the gas purity

Two isotherms using argon gas were performed in 2009. Figure 5 presents the gas temperature variations and the inner pressure changes during the second isotherm.

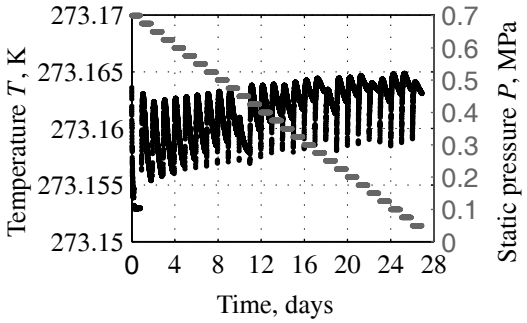

Figure 5: Gas temperature T and static pressure P variations during the second BCU3 isotherm performed at LNE-CNAM with argon

The right drawing of Figure 1 shows the thermostat used in order to control the temperature and the pressure near BCU3. The equipped resonator is positioned inside a pressure vessel where it is possible to make measurements from 0.05 MPa to 0.7 MPa.

Around this pressure vessel a thermal screen is used to control the inner temperature. A vacuum vessel surrounds this device and then, is immersed inside a Dewar flask containing a mix of ethanol and water ($T_{mix} < T_{TPW}$) to cool this system to T_{TPW}. We can obtain with this system a drift smaller than 0.1 mK/h. During the isotherms, the temperature is controlled with three Capsule Standard Platinum Resistance Thermometer (CSPRT) placed on different positions of the resonator shell.

Knowing very well the gas molar mass M, is one of the key point for getting a low uncertainty on k_B. Our gas handling system is equipped with a cold trap system which condenses gases into a liquid or solid for catching gases impurities different than argon (H_2O, Xe, Kr). Another device, a getter of gas particles, allows us to purify argon gas of other elements by adsorption (N_2, O_2, H_2O, THC, CO_2, H_2). Moreover, impurity measurements were realized; the presence of others elements could be estamed, 0.52 ppm for He and 0.29 ppm for Ne [2].
A continous argon flow renews the gas contained within the resonator. First of all neglected on the acoustic measurement, the effect of the gas flow was experimentally studied for different static pressures and corrected to zero-flow limit using an empirical function [2].

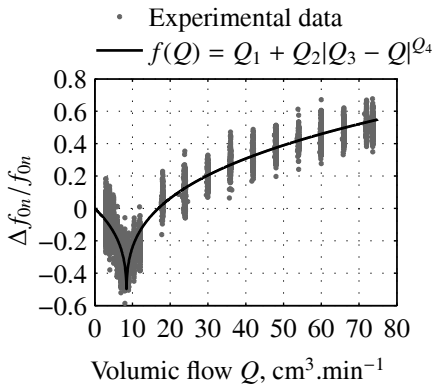

Figure 6: Gas flow effect on the acoustic measurement, at $P = 0.1$ MPa and $T = 273.16$ K. Coefficients Q_1, Q_2, Q_3 and Q_4 are ajusted using an optimization method

4 Data analysis

The previous step for determining u is to measure precisely the experimental resonant frequency. It is obtained fitting the experimental data with a Lorentzian function defined as

$$V(f) = \frac{iAf}{(f^2 - F^2)} + B + C(f - f_{0n}^e) + D(f - f_{0n}^e)^2, \quad (18)$$

where f is the source frequency, $V(f) \equiv X(f) + iY(f)$ is the complex signal detected by the lock-in amplifier, $F = f_{0n}^e + ig_{0n}^e\sqrt{f_{0n}^e/f}$, f_{0n}^e and g_{0n}^e are the experimental resonance frequency and the experimental half-width which best fit the experimental data. $X(f)$ and $Y(f)$ are respectively the experimental signal in-phase and quadrature-phase. The influence of the $V(f)$ definition on the determination of f_{0n}^e and g_{0n}^e was studing in this work, in particular, the number of data points using for the fit, the case when $\sqrt{f_{0n}^e/f} = 1$ and, simplifying $V(f)$ of it term D. Figure 7 shows typical raw signals measured for the acoustic mode 03.

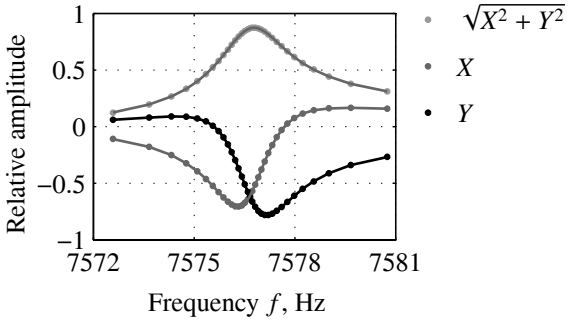

Figure 7: Typical raw signals for the acoustic mode 03. Data points correspond to the experimental signals, and solid lines to the computed signal magnitude

The next step consists in correcting $f_{0n}^e(P,T)$ of the disruptive effects described in section 2, in order to determine $u^2(P,T)$. Then, 2$^{\text{nd}}$ and 3$^{\text{rd}}$ polynomial fonctions are used for

extrapolating $u^2(P,T)$ to it zero pressure limit, as shown in Eq.(1) [2]. Figure 8 shows the comparison between the final values of k_B determined with two isotherms, using six radial modes for the first isotherm and four radial modes for the second, with the k_B CODATA recommanded value of 2006.

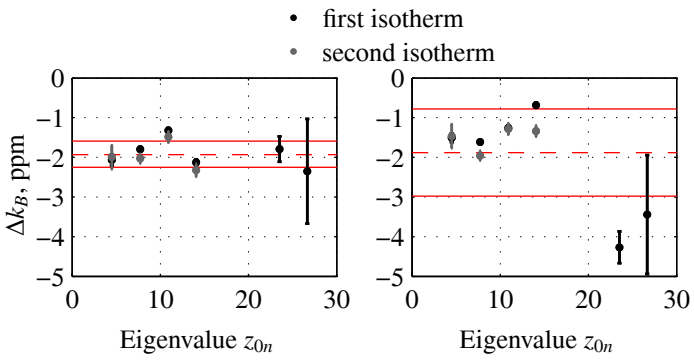

Figure 8: Final values of k_B, with uncertainty bars estimated from the fit at the zero-pressure limit, determined with the 2nd order polynomial function (left) and the 3rd order polynomial function (right), plotted as the fractional deviations from the 2006 CODATA value. Dashed red lines represent the k_B^{0n} average values of each chart, and full red lines the uncertainties

5 Conclusion

In this work realized at LNE-CNAM, the Boltzmann constant k_B was determining with an acoustical method consisting in measuring the speed of sound u in argon. The two isotherms yield the average value $k_B = 1.38064774\ (171) \cdot 10^{-23}\ \mathrm{J \cdot K^{-1}}$, i.e. with a relative standard uncertainty of $1.24 \cdot 10^{-6}$. This is the more accurate k_B determination made since the last two decade [3].
In 2011, the CODATA recommended a new value $k_B^{CODATA} = 1.3806488\ (13) \cdot 10^{-23}\ \mathrm{J \cdot K^{-1}}$, i.e. with a relative standard uncertainty of $0.91 \cdot 10^{-6}$.
Research on this topic is still in progress at LNE-CNAM. At present, isotherms using helium are performed with BCU3. As well, a 3.1 L resonator was build and will be use soon in a new experience, first with argon, then with helium.

Acknowledgments

The authors gratefully acknowledge Michael R. Moldover and James B. Mehl for sharing their long experience on the subject and their constant advice. Numerous persons contributed to this work. In particular, we would like to thank Roberto Gavioso, Paolo Alberto Giuliano Albo, Michael de Podesta, Robin Underwood and Gavin Sutton for the many discussions, the shared project results and years of collaboration. We also thank Michel Bruneau, Anne-Marie Bruneau and Cécile Guianvarc'h for providing acoustic expertises. We would not have been able to achieve these results without the support of Terry Quinn, Françoise Le Frious and Yves Hermier. We gratefully acknowledge funding under the French National Research Agency ANR and the EMRP programme of the European Union.

References

[1] 23rd General Conference on Weights and Measures, *Text of the resolutions adopted by the 23rd General Conference on Weights and Measures*,(2007)

[2] L. Pitre, F. Sparasci, D. Truong, A. Guillou, L. Risegari, M.E. Himbert, "Measurement of the Boltzmann constant k_B using a quasi-spherical acoustic resonator", *Int. J. Thermophys.* **32**, 1825-1886 (2011)

[3] M.R. Moldover, J.P. Trusler, T.J. Edwards, J.B. Mehl and R.S. Davis, "Measurement of the universal gas constant R using a spherical acoustic resonator", *J. Res. Natl. Bur. Stand.* **93**, 85-144 (1988)

[4] M.B. Ewing and M.L. McGlashan and J.P.M. Trusler, "The temperature-jump effect and the theory of the thermal boundary layer for a spherical resonator. Speeds of sound in argon at 273.16 K", *Metrologia* **22**, 93-102 (1986)

[5] B. Song and M.M. Yovanovich, "Correlation of thermal accommodation coefficient for'engineering'surfaces", *Proceedings of the Twenty-fourth National Heat Transfer Conference and Exhibition, Pittsburgh (USA), Aug. 9-12* **1**, 107-116 (1987)

[6] J.B. Mehl, M.R. Moldover and L. Pitre, "Designing quasi-spherical resonators for acoustic thermometry", *Metrologia* **41**, 295-304 (2004)

[7] C. Guianvarc'h, R.M. Gavioso, G. Benedetto, L. Pitre and M. Bruneau, "Characterization of condenser microphones under different environmental conditions for accurate speed of sound measurements with acoustic resonators", *Rev. Sci. Instrum.* **80**, 074901 1-074901 10 (2009)

[8] M. Bruneau, A.-M. Bruneau,Z. Skvor, P. Lotton, "An equivalent network modelling the strong coupling between a vibrating membrane and a fluid film", *Acta Acustica* **2**, 223-232 (1994)

[9] K.A. Gillis, H. Lin and M.R. Moldover, "Perturbations From Ducts on the Modes of Acoustic Thermometers", *J. Res. Natl. Inst. Stand. Technol.* **114**, 263-285 (2009)

[10] J.B. Mehl, "Acoustic Eigenvalues of a Quasispherical Resonator: Second Order Shape Perturbation Theory for Arbitrary Modes", *J. Res. Natl. Inst. Stand. Technol.* **112**, 163-173 (2007)

[11] L. Pitre, M.R. Moldover and W.L. Tew, "Acoustic thermometry: new results from 273 K to 77 K and progress towards 4 K", *Metrologia* **43**, 142-162 (2006)

[12] J.B. Mehl, "Spherical acoustic resonator: Effects of shell motion", *J. Acoust. Soc. Am.* **78**, 782-788 (1985)

[13] M. de Podesta, E.F. May, J.B. Mehl, L. Pitre, R.M. Gavioso, G. Benedetto, P.A. Giuliano Albo, D. Truong and D. Flack, "Characterization of the volume and shape of quasi-spherical resonators using coordinate measurement machines", *Metrologia* **47**, 588-604 (2010)